Asperity interaction and dependence of frequency-size distribution of earthquakes in brittle-ductile transition zone in Central Himalaya

Anil Tiwari[1], Ajay Paul[1], Rakesh Singh[2], and Rajeev Upadhyay[3]

[1]Wadia Institute of Himalayan Geology
[2]Graphic Era Hill University
[3]Kumaun University

November 23, 2022

Abstract

We explore the hypothesis that b-value act as stress meter which varies inversely with differential stress and decreases until it reached the depth of brittle-ductile transition. Correlation of seismogenic asperity and brittle-ductile contact (BDC) with b-value is of special interest. Lowest b- and Dc-values coincides with transition depth and interpreted as seismogenic asperities. Moderate ruptures (ML[?]5.0) nucleate in vicinity of transition zone where stress concentration is highest. We illustrate behavior of mid-crustal detachment and dependence of topographic elevation above Mid-Crustal Ramp (MCR). The depth 10-15 km is marked as MCR which coincides with fluids, seismogenic asperity and shows seismic clustering. The composite trend in abrupt escalation of b-value is observed at depth [?]12 km and [?]7 km for Garhwal and Kumaun region respectively. These depth ranges is demarcated as BDC which coincides with proposed MCR and exhibiting as an alarming asperity zone (12-15 km) for future great earthquake in Garhwal-Himalaya.

Asperity interaction and dependence of frequency-size distribution of earthquakes in brittle-ductile transition zone in Central Himalaya

Anil Tiwari[1, 3], Ajay Paul[1], Rakesh Singh[2], Rajeev Upadhyay[3]

[1]Wadia Institute of Himalayan Geology, Dehradun, India
[2]Department of Earth Sciences, Graphic Era Hill University, India
[3]Department of Geology, Kumaun University, Nainital, India

Corresponding author: Anil Tiwari (anilgeox93@gmail.com)

Key Points

- Three-dimensional spatio-temporal distribution of b-values along D_c-values is observed to identify seismogenic potential zone
- The BDC and associated seismogenic asperity is identified which coincides with MCR and considered as primary asperity for great earthquake
- Rheology transformation and seismogenic asperity governs the MCR geometry and tectonic-topographic control on the active fault zone

Abstract

We explore the hypothesis that b-value act as stress meter which varies inversely with differential stress and decreases until it reached the depth of brittle-ductile transition. Correlation of seismogenic asperity and brittle-ductile contact (BDC) with b-value is of special interest. Lowest b- and D_c-values coincides with transition depth and interpreted as seismogenic asperities. Moderate ruptures ($M_L \geq 5.0$) nucleate in vicinity of transition zone where stress concentration is highest. We illustrate behavior of mid-crustal detachment and dependence of topographic elevation above Mid-Crustal Ramp (MCR). The depth 10-15 km is marked as MCR which coincides with fluids, seismogenic asperity and shows seismic clustering. The composite trend in abrupt escalation of b-value is observed at depth ≈12 km and ≈7 km for Garhwal and Kumaun region respectively. These depth ranges is demarcated as BDC which coincides with proposed MCR and exhibiting as an alarming asperity zone (12-15 km) for future great earthquake in Garhwal-Himalaya.

Plain Language Summary

The continuous seismic monitoring indicates increase in stress accumulation in Garhwal-Kumaun, Central (NW) Himalaya. We observed more pronounced clustering of events and associated high stress accumulation in Chamoli-Rudraprayag region along the strike of Himalaya. The monitoring of this region is important because a strong earthquake Mb 6.3 (1999) was occurred in Chamoli zone of Garhwal region and several hundred people died with approximately 50,000 houses were damaged and over 2,000 villages were affected. Recently, after 1999 this periphery was triggered by moderate magnitude of M_L 5.7 earthquake. We find consistent results for various zones and observed that stress values vary inversely with the differential stress in the upper continental crust. The depth region 10-15 km indicates the presence of fluid, high stress accumulation and shows clustering in the association of surrounding faults and deformations. A well demarcation of Brittle-Ductile contact and associated asperity for future great earthquake is plotted which shows significant match of this depth ranges with moderate size of earthquake. We propose the location and building processes of MCR and associated superimposed layer which controls topography elevation in the region.

1. Introduction

The fundamental statistical analysis of frequency-magnitude distribution (Ishimoto and Iida, 1939; Gutenberg and Richter, 1944, 1954) in any region satisfies the relationship

$$\log_{10}N(M) = a - bM \qquad (1)$$

where ‘a’ and ‘b’ are constant and describes productivity parameter and relative size distribution slope respectively and N denotes total number of earthquakes with magnitude ≥M. The b-value is used for determine frequency of earthquake-size distribution and variation within the slope of power law i.e. low b-value means higher magnitude earthquake is predominant over low magnitude earthquake and vice-versa. The distribution of continuous stress accumulation along the fault-plane affects time of occurrence of next earthquake. Therefore it is necessary to know the spatio-temporal behavior of stress level in tectonic regime. It has been understood that different tectonic regime and associated structural characteristics yields variations in stress release: normal faults is associated with highest b-values, whereas reverse faults corresponds to lowest (Amelung and King, 1997; Schorlemmer et al., 2004; Kulhanek, 2005). Temporal variation in b-value appears to be associated with changes in local and regional stresses. In this study, the inverse relation between b-value and differential stress for continental crust has been verified. The relationship is carried out on regional scale to delineate different associated asperities.

Since 1944, depth-dependent b-value has been studied by many researchers (Guttenberg and Richter, 1944; Evernden, 1970; Wyss, 1973; Curtis, 1973; Mori and Abercrombie, 1997; Spada et al., 2013). The b-value is significantly termed as stress-meter for any region and interpreted as an indicator of heterogeneity in medium (Mogi, 1962; Kawamura and Chen, 2017). The pattern of depth distribution of local seismicity demarcates interface between brittle and ductile contact in seismogenic crust (Sibson, 1984; Amitrano, 2003; Spada et al., 2013). On a broad perspective, ratio of V_p/V_s also defines the behavior of brittle-ductile contact (BDC) and scale of rigidity within the crust. The stress gradient inferred by b-values controls seismicity and associated fracture density at brittle-ductile transition zone (Scholz, 1988; Doglioni et al., 2015). This paper defines the brittle-ductile transition zone in three different zones and associated seismogenic asperity along the strike of central-Himalaya. The thickness of brittle upper-crust is not uniform along the Main Central Thrust (MCT) and controls hypocenters of moderate size earthquakes within the transition zone.

A barrier along the fault plane which has significant resistance to slip in a highly stressed local area is termed as an asperity (Lay et al., 1982; Tormann et al., 2012). It has been plotted that highly stressed asperities coincides with zones of low b-value (Wiemer and Wyss, 1997). The earthquake rupture usually begins at an asperity and these barriers have significant amount of stress drop (Bouchon, 1997). Finding of seismogenic asperity zone and its interaction with surroundings is very important because it not only governs the significant aspects of earthquake ruptures but it may also be possible region where stress accumulates until it ruptures during a major earthquake. In this paper author demonstrates that asperities in fault zone corresponds to significantly low b- and D_c-values.

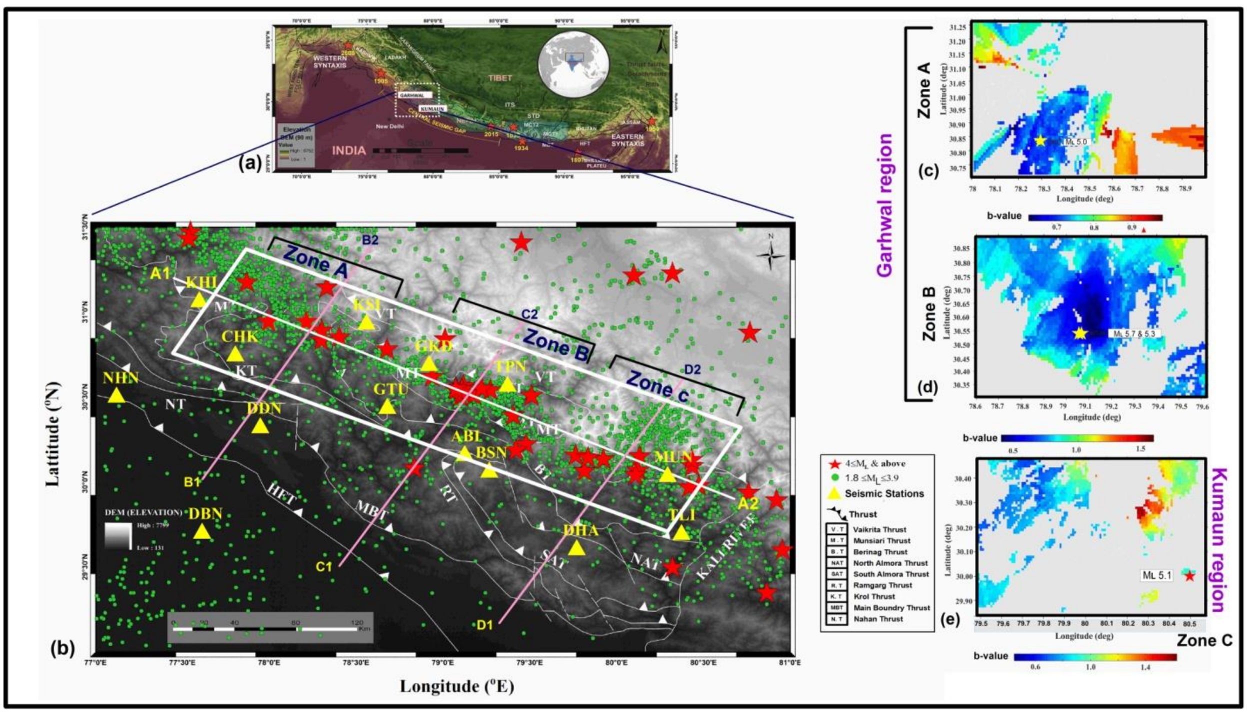

Figure 1. (a)The significant earthquakes of Himalayan Arc along major structures and tectonics (modified after Gansser, 1964; Valdiya, 1980b; Armijo et al., 1986; Bilham and Ambraseys, 2005; Kumar et al., 2010; Zhang et al., 2016). The study area (Garhwal-Kumaun Himalaya) located in CSG with no great earthquake, since last 20 decades. (b) Epicentral location map of local earthquakes (2007-2018) drawn on tectonic map of Garhwal-Kumaun region, with four profiles selected across and along the strike for seismic (A-A1, B-B1, C-C1 and D-D1), b-value cross-section and swath profile. (c-e) shows zone wise distribution (Zone A, B & C) and mapping of b-values on the tectonic map.

Study of stress level asperities in locked zone of Garhwal-Kumaun compressive regime of Central Seismic Gap (CSG) indicates observed variation in b-values with time, which shows significant decreasing trend for the period 2007-2013 (Negi and Paul, 2015). The Chamoli-Rudraprayag in Garhwal Himalaya and its adjoining region has experienced various earthquake swarms which may be precursor and preparation zone for moderate to great earthquake (Paul and Sharma, 2011; Singh et al., 2018). Due to this significant variation in seismically active region, it is necessary for continuous monitoring to study seismic parameters i.e. a-value, b-value and D_c (fractal dimension) to mitigate the probable seismic risk.

In this paper we describe the pattern of earthquake distribution, b-value and fractal analysis to understand the dynamics and stress condition of region in regional and local scale. We achieved a significant spatio-temporal behavior and depth dependence of b-value in the region. We have plotted b-value cross-section map for three different seismically active zones and identify seismogenic asperities and delineates its seismic characteristics. The location of low b-values coincides with low D_c-value reflects and interpreted as high-stressed asperities. Correlation of asperity zone and brittle-ductile transition with b-value has been achieved. We have illustrated the behavior of mid-crustal detachment beneath the Himalayan Seismic Belt (HSB) and dependence of topographic elevation due to change in depth of BDC.

2. Seismo-tectonics of Garhwal-Kumaun Himalaya

The Garhwal-Kumaun Himalaya lies in the western part of Central Seismic Gap (CSG) which is in between two major rupture zone i.e. 1905 kangra earthquake and 1934 Bihar-Nepal earthquake (Figure 1). The CSG is continuously acquiring strain and yields low to moderate magnitude of earthquakes with low stress drop, as a result large amount of internal stress is continuously being built up in this region to produce great earthquake(s) (Kayal, 2001; Gitis et al., 2008; Kumar et al., 2012; Singh et al., 2018; Paul et al., 2017, 2019). Khatri [1999] described that region has a potential of generating great earthquake and it is the most probable zone for future big earthquake with 52 % probability in a time window of 100 years. Since last 200 years CSG have not witnessed any major or great earthquake (>M 8) and the continuous process of acquiring strain energy marked the region as potential zone for next great earthquake

(Khatri, 1987). The region has experienced several major earthquakes in past, viz. 1803-Badrinath, 1816-Gangotri and 1867-Mussoori earthquakes (Oldham, 1883). In the last 3-4 decades region is visited by several moderate to strong earthquakes, (1991) Uttarkashi earthquake Mb 6.5, (1999) Chamoli-Garhwal earthquake Mb 6.3 (Kayal et al., 2003), (2007) Kharsali earthquake M 4.9 (Kumar et al., 2012), (6^{th} Feb 2017) Rudraprayag earthquake M 5.7 (present study) and (6^{th} Dec 2017) Rudraprayag earthquake M 5.3 (present study). The 6^{th} February 5.7 magnitude Rudraprayag earthquake (Mb 6.3) is the maximum recorded magnitude till now in our network since 1999 Chamoli-Garhwal earthquake which was followed by next moderate size of earthquake on 6^{th} December 5.3 magnitude in Rudraprayag province.

.

3. Data Analysis

The data used in present work studied for seismicity analysis and other seismic parameters which have been acquired by using fourteen broad band seismometers: ten stations from Garhwal network and four station of Kumaun network in Central Himalaya. The broad band stations which is deployed in Garhwal region are equipped with Trillium-240 seismometer whereas Kumaun network stations are equipped with Trillium-120 seismometer with high dynamic range (>138 db) with Centaur and Taurus Data acquisition system (DAS) respectively. Each station is consisting of standard frequency bandwidth range i.e.0.004-50 Hz, where three component data has been acquired in continuous mode at 100 samples per second at each station. High accuracy GPS synchronies the DAS clock every minute. The well located local-events are plotted on tectonic map of Garhwal Himalaya justified within the acceptable error bars (ERZ, ERH <5.0). The fresh data (2015-2018) is used and added in this study which was analyzed and processed using HYPO71 Program incorporated in SEISAN software (Lee and Lahr, 1975) at earthquake processing centre of the Wadia Institute of Himalayan Geology (WIHG), Dehradun, India.

This is for first time that the present seismicity, b- and D_c-value of region has been looked for more than 10 years continuous dataset which includes significant moderate size M_L 5.7, 2017 earthquake (since 1999) in the region. The data analysis for more than 3500 local events (2007 to 2018) indicate that majority of earthquakes are occurring in a narrow zone, south of MCT with magnitude range between 1.8 to 5.7. Current Status of the seismic network and previous study also suggests that, there is no major and strong event (Mag >6) in this region since 1999 till date.

4. Methodology

4.1 b-value Analysis and mapping

The spatial mapping of frequency-distributions of b-value has become a worldwide popular earthquake statistical analysis. The power-law for statistical distribution between magnitude of earthquakes and frequency of occurrence with the group of earthquakes is expressed in terms of Gutenberg–Richter relation (Gutenberg & Richter, 1944). The size distribution of earthquakes in the Earth's crust generally obeys this power law.

$$\log_{10} N(M) = a - bM \qquad (1)$$

The terms and constants of equation are defined in introduction. By mapping the spatial variation of b-value in entire region (29°–31.5°N; 77°–81°E), three zones has been identified on the basis of seismic clustering and low b-value characteristics (Figure 1 and 2 b-c).

The maximum-likelihood is most appropriate method as compared to least-square method (Hitara, 1989) and is applied in study to estimate b-value of the region (Aki, 1965). This method follows the mathematical relation and defined as

$$b = \frac{\log_{10} e}{M_a - M_c} \qquad (2)$$

Where M_a is the average magnitude and M_c is threshold magnitude above which the distribution of data is complete. We calculate b-values by giving sample size greater than 50 events (Nmin=50) above Mc. The M_c has been determined by applying goodness-of-fit method which is also called as maximum-curvature method (Wyss et al., 1999; Wiemer and Wyss, 2000). Mc is defined in present work as first magnitude bin at which residual falls below horizontal of 95% to 90% fit. The observed goodness-of-fit level of 95% to 90% (magnitude range, 1.8-5.7) defined Mc value of 1.8 for Zone A&B and Mc value of 2.4 for Zone-C for present seismicity catalogue. The aftershocks have been removed using declustering method given by Reasenberg [1985] before calculating the b-value. Further, b-values and standard-deviation have been achieved individually for all three zones by applying bootstrap method for computation, using software package ZMAP (Wiemer, 2001).

4.2 Fractal dimension

The scaling parameter for spatial distribution of earthquakes is termed as fractal dimension (D_c) (Mandlbrot, 1983). This power-law works as statistical tool and estimates the two-point spatial correlation for earthquake epicenters. The D_c-value describes earthquake's spatial randomness and clusterisation which helps in interpretation of seismic heterogeneity along the tectonic regime. The D_c-value for spatial distribution of earthquake is calculated using correlation integral method given by Grassberger and procaccia [1983] as:

$$\mathrm{D_{wr}} = \lim_{\mathrm{r}\to 0} \mathrm{Log}(\mathrm{C_r}) / \mathrm{Log_r} \qquad (3)$$

Where (C_r) is correlation function

$$\mathrm{C(r)} = \frac{2}{\mathrm{N(N-1)}} \mathrm{N}(\mathrm{R} < r) \qquad (4)$$

Where $\mathrm{N}(\mathrm{R} < r)$is the number of pair ($X_i$, X_j) with a smaller distance than angular distance (r). Kagan and Knopoff [1980] had described the correlation integral is related to standard correlation function given as:

$$\mathrm{C(r)} \sim \mathrm{r}^{\mathrm{D}} \qquad (5)$$

Here, D is typically termed as D_c-value. Author made a comparable work and carried out fractal dimension outline for whole region, zone-wise, year-wise and depth-wise also (Table S2-S4).

5. Results and Discussion

5.1 Spatial-temporal variation and depth correlation

A significant 3-D spatio-temporal distribution of b- and D_c-values is observed for entire 12 years continuous dataset. The results are well constrained at 5-20 Km with less uncertainties. The b-value is found to be 0.835 ± 0.02, while a-value is calculated 5.01 for whole region (Table S2). In a tectonically active region, observed b-value is commonly close to 1.0 but varies between 0.5 and 1.5. Earlier workers have also estimated b-values in Himalaya that ranges between 0.60-1.05 (Pacheco et al. 1992; Wiemer and Wyss, 1997; Pandey et al., 1999; Kayal, 2001; Ghosal et al., 2012; Prasath et al., 2019). The D_c-value is estimated 1.53 ± 0.03 and fractal scaling range found between 11.49 and 56.86 km for whole region.

By mapping the spatial variation of b value in entire region, three zones (Zone-A, Zone-B and Zone-C) has been identified on the basis of events clustering and b-value characteristics (Table S2). The obtained b-values for Zone-A (Uttarkashi region), Zone-B (Chamoli-Rudraprayag region) and Zone-C (Kumaun region) are 0.737 ± 0.04, 0.702 ± 0.03 and 0.97 ± 0.07 respectively. We have plotted cross-section of stress map across and along the strike, which clearly depicts Zone-B accumulates more stress and highly clustered by seismicity with recently occurred M 5.7 earthquake (Figure 2 & S2). The relative increase in stress and recent seismic activity with this moderate size of earthquake in Zone-B probably indicates accumulation of high stress as compared to other Zone A & C in entire region.

We have estimated b- and D_c-value separately for MCT zone and south of MCT (Figure S3, S4 and table S2). The b- and D_c-values are found 0.755 ± 0.03 and 1.46 ± 0.04 respectively for MCT zone, 0.705 ± 0.03 and 1.36 ± 0.01 respectively for south of MCT. The inferences based on the spatial variation indicate that south of MCT (inner Lesser Himalaya) is more pronounced by homogenous seismic distribution and accumulates high stress than MCT zone along the strike. The thrust system of lesser Himalaya (south of MCT) is more seismically active and accommodates most of the stress due to convergence along the strike of Himalaya (Kayal et al., 2003a,b; Bai et al., 2016). We observed that low D_c-value always coincides with high stress field (Table S2-S4) and suggests the pattern of seismic distribution. The highest D_c-value in Zone-A suggests the heterogeneity of earthquake density and zone-B illustrates lowest D_c-value which indicates homogeneity of earthquake density with clusterisation (figure 2b and Table S2).

The b-value varies inversely with differential stress and effective stress in the continental crust (Scholz, 2015). It is acknowledged that differential stress in upper crust increases until it reached the depth of brittle-ductile transition zone at which ductile mechanisms begin to operate, thereafter differential stress decays (Connolly and Podladchikov, 2004). The brittle fracture dominantly distributed in the upper crust while ductile flow is pronounced in the Earth's lower crust (13km depth), rupture activity in the crust is widely affected by this scale (Lei and Kusunose, 1999). We individually investigated and mapped 1D b-value with depth cross-section for each block of active region (Figure 2 and S4). The obtained numerical values are in agreement of decrease in b-value with increase in depth, which is controlled by differential stress. The region in between 10-15 km depth shows computed result of relatively low b-value

0.647 ± 0.03 for entire region (Table S3) which is an indication of high strain accumulation. We have obtained depth-wise as well as spatio-temporal D_c-value (0.83 to 1.89) for entire region. (Table S3, S4). It has been observed that low D_c-value suggests high permeability and presence of fluids in fault plane as well as in its surrounding area which contributes in decaying of effective stress (Barton et al., 1999; Monsalve et al., 2008; Singh et al., 2008). The low D_c-value of 0.83 ± 0.01 at 10-15 km depth for entire region (Table S3) indicates the presence of fluid and showing seismic clustering in association of surrounding faults and deformations.

A high conductivity, low velocity layer along low coefficient fiction value is observed beneath the Garhwal Himalaya which was predicted as a free fluid source (Rawat et al., 2014; Prasath et al., 2017). It has been interpreted as 1999 Chamoli earthquake influenced by free fluids and previous study also reported the presence of fluid evident by high Vp/Vs values beneath the Chamoli region in Garhwal-Himalaya (Mahesh et al., 2012; Caldwell et al., 2013; Rawat et al., 2014). We suggest the presence of such trapped fluids along the detachment plane around MCR structure which alters vertical distribution and may lead in decay of differential stress with increase in b-value. Decrease in D_c-value with b-value may be the indicator for high stress developer along the fault to produce large size earthquake. The temporal range of 2015-2018 shows low b-and Dc-value (Table S4). This period observed large frequency of moderate size earthquakes, hence shows high stress in the region.

5.2 Mapping brittle-ductile transition and associated asperities along the thrust zone

Seismogenic asperity is the area of relatively high accumulation of shear and normal stresses along the fault zone. Elucidating the position of seismogenic asperity is important to understand significant aspects of earthquake ruptures and its nucleation for future large earthquake. We have examined the asperities in fault zone and are mapped anomalously by low b-value distribution. The hypocenters of majority of moderate size earthquake since 2007 as well as foci of 1991 Uttarkashi and 1999 Chamoli strong earthquakes coincide with these asperities and zone of low b-value, indicates release of continuously accumulating stress. The lowest spatial as well as depth wise b-value is found in Zone-B and marked this area as a seismogenic asperity zone for future large earthquake.

In Figure 2, depth estimation of b-value suggests that Zone-B shows high degree of variation as compared to Zone-A and Zone-C. The Zone-B depicts minimum b-value <

0.7 at depth ≈12-14 km. Interestingly two moderate size earthquakes of M_L5.7 (6th Feb 2017) and M_L5.3 (6th Dec 2017) magnitudes occurred in this region with focal depth 14.6 km and 13.5 km respectively. In addition, majority of moderate size of earthquakes were occurred in a narrow zone of this region with depth range 12-15 km (Table S5). The trend in sudden escalation of b-value at depth ≈12 km indicates that Zone-B is behaving as BDC and 12-15 km as asperity zone for significant ruptures, whereas Zone-A shows high stress gradient of b-value with approximately similar depth asperities as of Zone-B (Figure 2). The zone-C shows anomalous behavior and depicts ≈7 km depth as BDC which coincides with low b-value and below it b-value increases progressively. The majority of small to moderate size earthquake with depth range 7-10 km occurred within asperity zone in Zone-C (Table S5). The shallow crustal depth indicates highly heterogeneous medium with high differential stress above ≈12 km for Zone A&B and ≈7 km for Zone-C.

We suggest that fractures are not closely packed in heterogeneous medium because of low stress condition. Even if rupture initiates in heterogeneous medium, fracture or weak zone do not easily propagate from one fracture to another because of loosely packed density, hence no moderate and strong earthquake occurred in shallow depth. On the other hand, ductile-zone is dominantly distributed by closely packed fracture density because of high stress and plastic behavior of medium. If rupture initiates in ductile-zone it propagates to a far extent because of high density of fractures and homogenous distribution of stress which may lead other fractures to trigger in medium. Hence, rupture propagation in ductile zone develops numerous moderate size of earthquake with low b- and D_c-value in lower crustal-depth because of uniform stress accumulation. Scholz [1990] observed that 10-15 Km depth is widely accepted and generally corresponds to transition zone from unstable friction to stable friction of the crust. Manning & Ingebritsen [1999] also pointed that 12-13 Km is a characteristic scale and significant boundary in geothermics and crustal permeability. Hence, Major rupture ceases in heterogeneous medium above BDC which coincides with low lithospheric pressure.

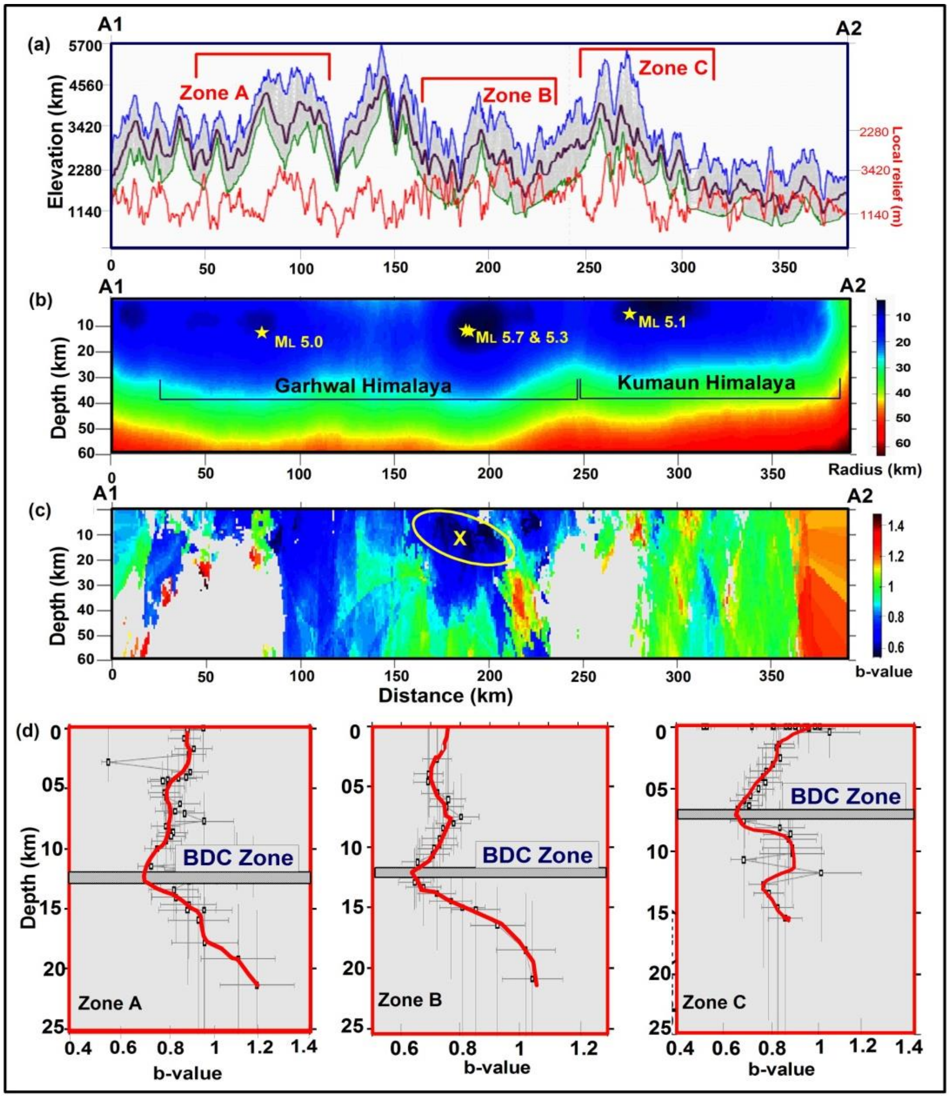

Figure 2. (a) The swath profile depicts Maximum, Minimum and Mean elevation with local relief along the strike of Himalaya which shows low elevation in Zone-B and highest at Zone-C. (b) It shows clusterization of local events which is dominantly present at Zone-B. (C) Shows b-value mapping depth cross section along the strike, which depicts Zone-B accumulates more stress and recently triggered by M 5.7 earthquake. Yellow elliptical circle (X) indicates dip direction of stress zone towards Zone-C i.e Kumaun Himalaya. (d) The swath profile along the strike shows topographic elevation varies with change in brittle-ductile contact (BDC) depicts tectonic control on topography.

5.3 Behavior of mid-crustal detachment beneath the HSB

The Geodetic and microseismic observation shows that MCR accumulates strain and stress beneath the higher Himalaya (Pandey et al., 1995: Arora et al., 2012). We suggest that seismicity and stress level distribution in brittle-ductile transition zone is a good proxy for presence of MCR and associated structures along HSB. Based on previous studies, decollement layer in Sub-Himalaya is present beneath 5-6 km thick Siwalik sediments (Delcaillau, 1986; Shelling and Arita, 1991). The MFT and MBT are rooted into decollement which indicates continuation of detachment beneath the Sub-Himalaya. The focal mechanisms of great to moderate-size earthquakes reveal that northward flattening of detachment plane (dip 2^0-4^0) beneath the lesser Himalaya. Further towards north in the vicinity of MCT beneath inner lesser Himalaya, plane of detachment steepens with dip of 16^0 and develops a ramp structure (Ni and Barazangi, 1984, Caldwell et al., 2013).

Seismic cross-section provides the evidence of seismic clustering with high stress accumulation in the vicinity of MCR but detachment with flat decollement does not correspond to same. The structural cross sections are shown (Figure 3) with depth variation in geometry of detachment plane. Author suggests the high stress asperity and associated ductile behavior of rock beneath the HSB controls and changes the geometry of detachment plane which steepens it and develops a ramp. Geometrical changes along the plane of detachment build locked patches which get influenced in high stress zone along the MCR. This locked portion and associated zone further superimpose by incompetent ductile layer during inter-seismic and aseismic slip. The superimposition of layers associated with ramp develops a duplex structure and the roof thrust which may get influenced in the proximity of brittle-ductile transition. We have compared the association of MCR in three different adjacent zones. Based on section 5.1 and table S2 we observed low D_c-value of 0.83 ± 0.01 at 10-15 km depth for whole region may indicates the presence of fluid and showing clustering in association of surrounding faults and deformations. We suggest the depth of MCR is 10-15 km from crustal surface in Garhwal region. The position of ramp shows correspondence with brittle ductile contact, stress variation, seismogenic asperity and hypocenters of moderate size earthquakes. Whereas inferences based on magneto-telluric and other studies on Garhwal region states that depth of ramp is 8-13 km (Rawat et al., 2014), 15-20 km (Srivastava and Mitra, 1994) and 10-20 km (Caldwell et al., 2013) . Based on earlier studies, the associated duplex structure is traced in high stress asperity zone within the ductile medium (Figure 3). We suggest area and location of MCR and associated duplex are controlled by rheology transformation from ductile to brittle along the MHT.

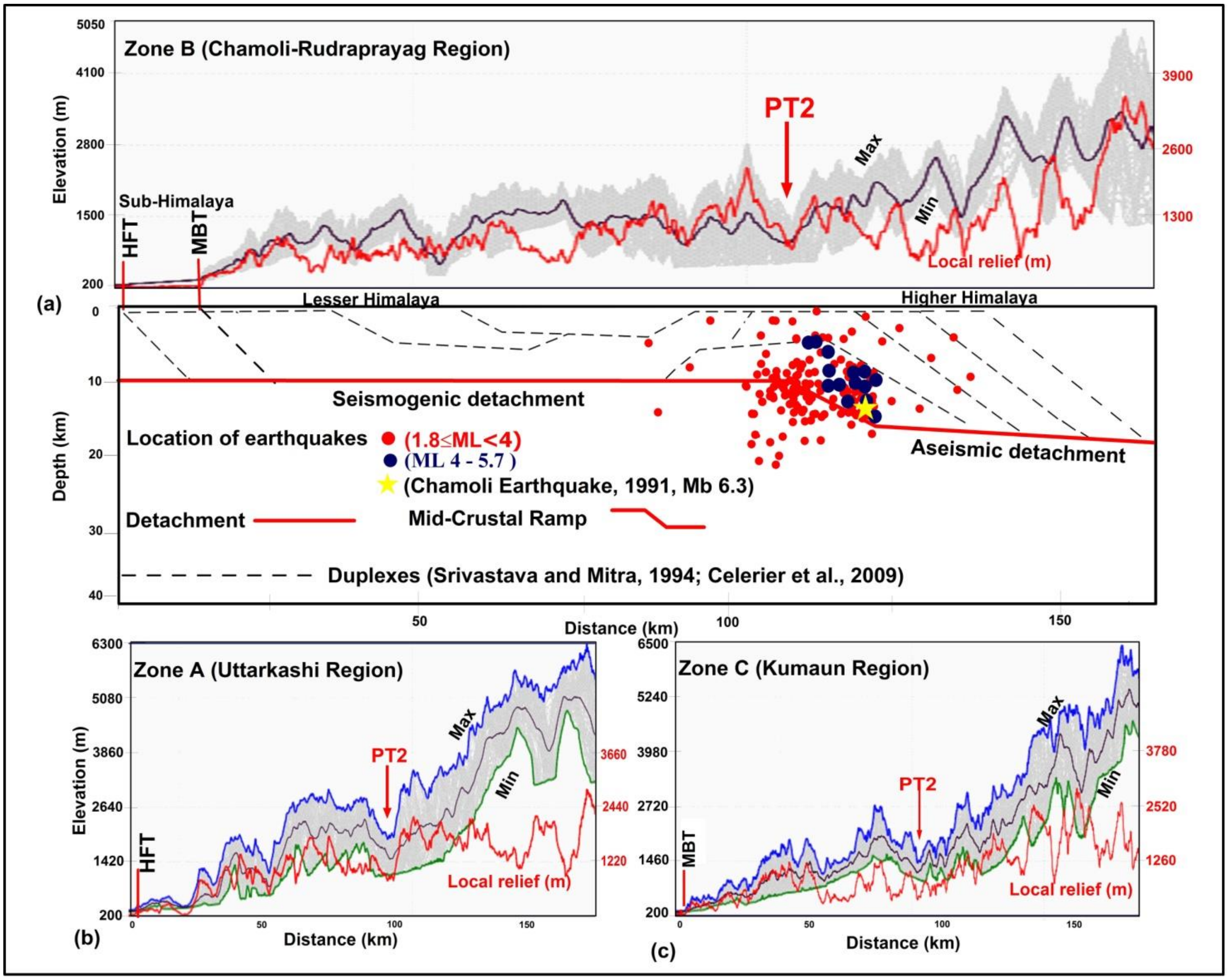

Figure 3. The Physiographic Transition (PT2) on swath profiles are observed for three different zones along with the MHT, MCR and duplex structure.

5.4 Tectonic and topographic control on active fault zone along the Himalayan strike

The orogenic belts of Himalaya are probably governed by northward movement of Indian plate towards Eurasian plate and controls the lateral changes along the strike in fold-and-thrust belts that affects elevation and basement decollement layers. The pattern of micro-seismicity and associated cluster along the HSB coincide with high elevation topography. The elevation difference corresponds to higher erosion rate with rock uplift (Lave and Avouac, 2001; Herman et al., 2010). The possibilities of anomalous behavior of topography could be the superimposition and growth of duplex above mid-crutal ramp (DeCelles et al., 2001; Avouac, 2003; Gao et al., 2016), thrusting above steep detachment plain (Lave and Avouac, 2001) and occurrence of out-of-sequence thrusting (Hodges et al., 2004). The study of tectonic and topography anomaly on the active fault zone is important for earthquake related hazards.

Plotting of swath profiles along the Himalayan strike states that depth variation in transition zone controls local topographic elevation and a locus of crustal thickening and shortening. The swath profile in three different zone shows a similar trend of PT2 feature with abrupt escalation in elevation along the Himalayan strike (Figure 3). The consistency of PT2 path at the foot of HHC supports the presence of MCR along HSB beneath the NW Himalaya. The inferences based on low b- and D_c-value depicts that Zone-B shows low elevation topography as compared to Zone A and C (Figure 2). The BDC is deeper in Zone-B and depth variation of b-value also shows low angle slope which indicate low stress gradient as compared to zone A and C. The Zone-C shows highest elevation topography and depicts shallowest brittle ductile transition zone with high stress gradient. Hence, we can observe that BDC is located significantly deeper in Garhwal region of Zone-B and shallower at Kumaun region of Zone-C. The possibilities of these anomalies are due to thrusting and growth of duplex in brittle ductile transition zone along the MCR. We suggest that location of transition zone coincide with low b- and D_c-values and associated seismogenic asperities govern the tectonic and topographic control on the active fault zone along the strike of Himalaya.

6 Conclusions

The continuous seismic monitoring provides the opportunity to study and analyze spatio-temporal b-value, fractal dimension and its dependence with depth in CSG. The analysis leads to following conclusions:

1. The b-value varies inversely with differential stress until it reached the depth of BDC.
2. The high stress asperity zone is found in Zone-B and verified its possible association with shallow depth inferred ruptured areas in Garhwal Himalaya.
3. The inner lesser Himalaya (south of MCT) is more seismically active which accommodates most of the stress with low D_c-value than MCT zone.

4. Significant change is observed in stress gradient at ≈12 Km and ≈7 km for Garhwal and Kumaun respectively, which we interpret as brittle ductile-transition and coincides with seismogenic asperity.
5. Stronger to great earthquake can occur at shallower depth below BDC in CSG.
6. Seismogenic asperity within brittle-ductile transition controls the rupture and amount of interseismic strain against the locked portion.
7. We predict that rheology transformation from ductile to brittle governs the position of MCR (10-15 km) and associated duplex along the MHT.
8. The swath profile confirms the consistency of PT2 path and supports the presence of MCR along the HSB. The associated BDC and seismogenic asperity at MCR controls the tectonic-topographic development on active thrust zone along the strike of Himalaya.

.

Acknowledgement

The authors are grateful to Dr. Kalachand Sain, Director, Wadia Institute of Himalayan Geology (WIHG), Dehradun for providing facilities and motivation to carry out this work. Our sincere thanks to the Ministry of Earth Science and Department of Science and Technology, New Delhi for generous financial assistance towards sponsoring the project and seismic network installation in NW Himalaya. Prof. H.K Gupta is sincerely acknowledged for valuable suggestion and comment. We are thankful to Dr Arun Prasath, Dr Sundeep Chabak for their support in discussion and Ms Jyoti Tiwari is acknowledged for improvement of manuscript. The present authors certify that they have no financial interest in the subject matter or materials discussed in this manuscript. The additional figures, tables and data used in this study are provided as supporting information. Consent from the corresponding author is needed to use the data set for any future publication.

Data related to this paper is generated and processed by Author (AT): The data July 2007 to May 2015 has been reprocessed and used in this study. The data 2015 to 2018 is newly generated and processed by Author at WIHG, Dehradun.

Data related to this paper is available and can be downloaded from the following link (http://dx.doi.org/10.17632/257pzrpdzd.3).

References

Aki, K. (1965), Maximum likelihood estimate of b in the formula log N = a-bM and its confidence limits, *Bull. Earthquake Res. Inst. Univ. Tokyo., 43*, 237–239.

Amelung, F., and G. King (1997), Earthquake scaling laws for creeping and non-creeping faults, *Geophys. Res. Lett., 24* (5), 507-510.

Amitrano, D. (2003), Brittle-ductile transition and associated seismicity: Experimental and numerical studies and relationship with the b value, *J. Geophys. Res., 108*, 2044.

Arora, B. R., V. K. Gahalaut, and N. Kumar (2012), Structural control on along-strike variation in the seismicity of the northwest Himalaya, *J. Asian Earth Sci., 57*, 15–24.

Armijo, R., P. Tapponnier, J. L Mercier, and T. L Han (1986), Quaternary extension in southern Tibet: Field observations and tectonic implications, *J. Geophys. Res., 91*(B14), 13803–13872.

Avouac, J.P. (2003), Mountain building, erosion, and the seismic cycle in the Nepal Himalaya, *Adv. in geophys., 46*, 1-80.

Barton, D. J., G. R. Foulger, J. R. Henderson, and B. R. Julian (1999), Frequency-magnitude statistics and spatial correlation dimensions of earthquakes at Long Valley Caldera, California, *Geophys, J. Int., 138*, 563–570.

Bai, L., H. Liu, J. Ritsema, J. Mori, T. Zhang, Y. Ishikawa, and G. Li (2016), Faulting structure above the Main Himalayan Thrust as shown by relocated aftershocks of the 2015 Mw7.8 Gorkha, Nepal, earthquake, *Geophys. Res. Lett., 43*, 637– 642, doi:10.1002/2015GL066473

Bilham, R., and N. Ambraseys (2005), Apparent Himalayan slip deficit from the summation of seismic moments for Himalayan earthquakes, 1500–2000, *Cur. Sci., 88*, 1658–1663.

Bouchon, M. (1997), The state of stress on some faults of the San Andreas system as inferred from near-field strong motion data, *J. Geophys. Res., 102*, 11,731– 11,744.

Caldwell, W. B., S. L. Klemperer, J. F. Lawrence, and S. S. Rai, (2013), Characterizing the Main Himalayan Thrust in the Garhwal Himalaya, India with receiver function CCP stacking. *Earth Planet. Sci. lett., 367*, 15–27.

Celerier, J., T. M. Harrison, A. A. G. Webb, and A. Yin (2009), The Kumaun and Garwhal Lesser Himalaya, India: Part 1. Structure and stratigraphy, *Bull. Geol. Soc. Am., 121*, 1262-1280.

Connolly, J. A. D., and Y. Y. Podladchikov (2004), Fluid flow in compressive tectonic settings: Implications for mid-crustal seismic reflectors and downward fluid migration, *J. Geophys. Res., 109*, B04201, doi:10.1029/2003JB002822.

Curtis, J. W. (1973), A magnitude domain study of the seismicity of Papua, New Guinea, and the Solomon Islands, *Bull. Seismol. Soc. Am., 63* (3), 787–806.

DeCelles, P.G., D.M. Robinson, J. Quade, T.P. Ojha, C.N. Garzione, P. Copeland, and B.N. Upreti (2001), Stratigraphy, structure, and tectonic evolution of the Himalayan fold-thrust belt in western Nepal, *Tectonics., 20*, 487–509.

Delcaillau, B. (1986), Dynamique et evolution morphostructurale du piémont frontal de l'Himalaya: les Siwaliks du Népal oriental, *Revue géologie Dynamique géographie Physique.*, *27*, 319-337.

Doglioni C., S. Barba, E. Carminati and F. Riguzzi (2015), Fault on-off versus strain rate and earthquakes energy. *Geosci. Front.*, *6*, 265–276.

Evernden, J.F. (1970), Magnitude versus yield of explosions, *J. Geophys. Res.*, *75*, 1028-32.

Gansser, A. (1964), Geology of the Himalayas. Wiley-Interscience, New York., 289.

Gao, R., Lu, Z. W., Klemperer, L., Wang, H. Y., Dong, S. W., Li, W. H., & Li, H. Q (2016), Crustal-scale duplexing beneath the Yarlung Zangbo suture in the western Himalaya, *Nat. Geosc.*, *9*(7), 555–560, https://doi.org/10.1038/NGEO2730.

Ghosal, A., U. Ghosh, and J. R. Kayal (2012), A detailed b-value and fractal dimension study of the March 1999 Chamoli earthquake (Ms 6.6) aftershock sequence in western Himalaya, *Geom. Natural Haz. and Risk.*, *3*(3), 271–278.

Gitis, V., E. Yurkov, B. Arora, S. Chabak, N. Kumar, and P. Baidya (2008), Analysis of seismicity in North India, *Russ. J. Earth Sci.*, *10*,ES5002, DOI: 10.2205/2008ES000303.

Grassberger, P., and I. Procaccia (1983), Characterization of strange attractors, *Phy. Rev. Lett.*, *50*(5), 346.

Gutenberg, B., and C. F. Richter (1944), Frequency of earthquakes in California, *Bull. Seismol. Soc. Am.*, *34*, 185–188.

Gutenberg, B. and C. F. Richter (1954), "Seismicity of the Earth and Associataed Phenomena", *Princeton University Press, Princeton, NJ, USA.*

Herman, F., et al. (2010), Exhumation, crustal deformation, and thermal structure of the Nepal Himalaya derived from the inversion of thermochronological and thermobarometric data and modeling of the topography, *J. Geophys. Res.*, *115*, B06407, doi:10.1029/2008JB006126.

Hirata T. (1989), A correlation between the b-value and the fractal dimension of earthquakes, *J. Geophys. Res.*, *94*:7507-7514.

Hodges, K. V., C. Wobus, K. Ruhl, T. Schildgen, and K. Whipple (2004), Quaternary deformation, river steepening, and heavy precipitation at the front of the Higher Himalayan ranges, *Earth Planet. Sci. lett.*, *220*(3–4), 379–389.

Ishimoto, M., and K. Iida (1939), Observations sur les séismes enregistrés par le microsismographe construit dernièrement (in Japanese with French abstract), *Bull. Earthquake Res. Inst. Univ. Tokyo.*, *17*, 443–478.

Kagan, Y. Y., & L. Knopoff (1980), Spatial distribution of earthquakes: The two-point correlation function, *Geophys. J. Int.*, *62*(2), 303–320.

Kawamura, M., and K. H. Chen (2017), Influences on the location of repeating earthquakes determined from a and b value imaging, *Geophys. Res. Lett.*, *44*, 6675– 6682, https://doi.org/10.1002%2F2017gl073335, https://doi.org/10.1002/2017gl073335.

Kayal, J.R. (2001). Microearthquake activity in some parts of the Himalaya and the tectonic model, *Tectonophysics.*, *339*, 331-351.

Kayal, J. R., S. Ram, O. P. Singh, P. K. Chakraborty, and G. Karunakar (2003a), The March 1999 Chamoli earthquake in the Garhwal Himalaya: Aftershock characteristics and tectonic structure, *J. Geol. Society of India.*, *62*(5), 558–580.

Kayal, J. R., S. Ram, O. P. Singh, P. K. Chakraborty, and G. Karunakar (2003b), Aftershocks of the March 1999 Chamoli earthquake and seismotectonic structure of the Garhwal Himalaya, *Bull. Seismol. Soc. Am.*, *93*(1), 109–117.

Khattri, K.N. (1987), Great earthquakes, seismicity gaps and potential for earthquake disaster along the Himalaya plate boundary, *Tectonophysics.*, *138*, 79 - 92.

Khattri, K. N. (1999), Probabilities of occurrence of great earthquakes in the Himalaya, *Proc. Indian Acad. Sci. (Earth Plan. Sci.).*, *108* (2), 87-92.

Kulhanek, O. (2005), Seminar on b-value Prague Centre of Mathematical Geophysics, Meteorology, and their Applications (MAGMA), Charles University, Prague, Czech.

Kumar, A., H. Mittal, R. Sachdeva, and A. Kumar (2012), Indian Strong Motion Instrumentation Network, *Seismol. Res. Lett.*, *83* (1), 59-66.

Kumar, S., S. G. Wesnousky, R. Jayangondaperumal, T. Nakata, Y. Kumahara, and V. Singh (2010), Paleoseismological evidence of surface faulting along the northeastern Himalayan front, India: Timing, size, and spatial extent of great earthquakes, *J. Geophys. Res. Solid Earth.*, *115*(B12), B12422. https://doi.org/10.1029/2009JB006789.

Lave´, J., and J. P. Avouac (2001), Fluvial incision and tectonic uplift across the Himalayas of central Nepal, J. *Geophys. Res. Solid Earth.*, *106*(B11), 26561–26591.

Lay, T., H. Kanamori, and L. J. Ruff (1982), The asperity model and the nature of large subduction zone earthquakes, *Earthquake Prediction Res.*, *1*, 3–71

Lee, W.H.K., and J.C. Lahr., (1975), HYPO71-revised: a computer Himalaya, India, *Bull. Geol. Soc. Am.*, *110* (8), 1010-1027.

Mandelbrot, B.B. (1983), The fractal geometry of nature. *New York: W.H. Freeman and Company*, *173*, 51.

Manning, C.E., and S.E. Ingebritsen (1999), Permeability of the continental crust—the implications of geothermal data and metamorphic systems, *Rev. Geophys.*, *37*, 127–150.

Monsalve, G., A. Sheehan, C. Rowe, and S. Rajaure (2008), Seismic structure of the crust and the upper mantle beneath the Himalayas: Evidence for eclogitization of lower crustal rocks in the Indian Plate, *J. Geophys. Res.*, *113*, B08315, doi 10.1029/2007JB005424.

Mogi, K. (1962), Study of elastic shocks caused by the fracture of heterogeneous materials and its relations to earthquake phenomena, *Bull. Earthq. Res.*, *40* (1) 125-173.

Mori, J., and R. Abercrombie (1997), Depth dependence of earthquake frequency–magnitude distributions in California: Implications for rupture initiation, *J. Geophys. Res.*, *102*(B7), 15081–15090.

Negi, S.S., and A. Paul (2015), Space Time Clustering Properties of Seismicity in the Garhwal-Kumaun Himalaya, India, *Him. Geol.*, *36* (1), 91-101.

Ni, J., M. Barazangi (1984), Seismotectonics of the Himalayan Collision Zone' Geometry of the Underthrusting Indian Plate Beneath the Himalaya, *J. Geophys. Res.*, *89*(B2), 1147-1163.

Oldhman, T. (1883), A catalogue of Indian earthquakes, *Mem. Geol. Survey of India*, *19*, 3, 493-503.

Pacheco, J. F., C. H. Scholz, and L. R Sykes (1992), Changes in frequency–size relationship from small to large earthquakes, *Nature.*, *355*(6355), 71–73.

Pandey, M. R., R. P. Tandukar, J. P. Avouac, J. Lavé, J. P. Massot (1995), Interseismic strain accumulation on the Himalayan crustal ramp (Nepal), *Geophys. Res.Lett.*, *22*(7), 751-754.

Pandey, M. R., R. P. Tandukar, J. P. Avouac, J. Vergne, T. He´ritier (1999), Seismotectonics of Nepal Himalayas from a local seismic network. *J. Asian Earth Sci.*, *17*, 703 - 712.

Paul, A., and M.L. Sharma (2011), Recent earthquake swarms in Garhwal Himalaya: a precursor to moderate to great earthquakes in the region. *J. Asian Earth Sci.*, *42*, 1179–1186.

Paul, A., and R, Singh (2017), Relevance of seismicity in Kumaun-Garhwal Himalaya in context of recent 25th April 2015 Mw7. 8 Nepal earthquake, *J. Asian Earth Sci.*, *141*, 253-258.

Paul, A., A. Tiwari, and R. Upadhyay (2019), Central Seismic Gap and Probable zone of large earthquake in North West Himalaya, *Him. Geol.*, *40* (2), 199 – 212.

Prasath, R. A., A. Paul, and S. Singh (2017), Upper crustal stress and seismotectonics of the Garhwal Himalaya using small-to moderate earthquakes: Implications to the local structures and free fluids, *J. Asian Earth Sci.*, *135*, 198–211.

Prasath, R.A., A. Paul, and S. Singh (2019), Earthquakes in the Garhwal Himalaya of the Central Seismic Gap: A Study of Historical and Present Seismicity and Their Implications to the Seismotectonics, *Pure App. Geophys.*, *176*, 4661–4685.

Rawat, G., B. R. Arora, and P. K. Gupta (2014), Electrical resistivity cross-section across the Garhwal Himalaya: Proxy to fluid seismicity linkage, *Tectonophysics.*, *637*, 68–79.

Reasenberg, P. (1985), Second-order moment of central California seismicity, 969–1982, *J. Geophys. Res.: Solid Earth.*, *90*(B7), 5479–5495.

Schelling, D., and K. Arita (1991), Thrust tectonics, crustal shortening, and the structure of the far-eastern Nepal, Himalaya, *Tectonics.*, *10*, 851, 10.1029/91TC01011

Scholz, C.H. (1990), The mechanics of earthquakes and faulting: Cambridge, *Cambridge University Press*, 439 .

Scholz, C. H. (1988), The brittle-plastic transition and the depth of seismic faulting, *Geologische Rundschau.*, *77*, 319–328.

Scholz, C. (2002), The Mechanics of Earthquakes and Faulting, 2nd ed, *Cambridge University Press*, New York.

Scholz, C. H. (2015), On the stress dependence of the earthquake b value, *Geophys. Res. Lett.*, *42*, 1399– 1402, doi:10.1002/2014GL062863.

Schorlemmer, D., S. Wiemer, and M. Wyss (2004), Earthquake statistics at Parkfield: 1. Stationarity of b values, *J. Geophys. Res.*, *109*, B12307, doi:10.1029/2004JB003234.

Sibson, R. H. (1984), Roughness at the Base of the Seismogenic Zone: Contributing Factors, *J. Geophys. Res. Atmospheres.*, *89*(NB7):5791-5799.

Singh, C., P. M. Bhattacharya, and R. K. Chadha (2008), Seismicity in Koyna-Warna reservoir site in western India: fractal and b-value mapping. *Bull Seismological Soc Am., 98*, 476-482.

Singh, R., R.A. Prasath, A. Paul, and N. Kumar (2018), Earthquake swarm of Himachal Pradesh in northwest Himalaya and its seismotectonic implications, *Phys. Earth Planet. Inter., 275* , 44-55.

Singh, R., A. Paul, A. Kumar, P. Kumar, and Y. P. Sundriyal (2018), Estimation and applicability of attenuation characteristics for source parameters and scaling relations in the Garhwal Kumaun Himalaya region, India, *J. Asian Earth Sci., 159*, 42-59.

Spada, M., T. Tormann, S. Wiemer, and B. Enescu (2013), Generic dependence of the frequency-size distribution of earthquakes on depth and its relation to the strength profile of the crust, *Geophys. Res. Lett., 40*, 709– 714, doi:10.1029/2012GL054198

Srivastava, P., and G. Mitra (1994), Thrust geometries and deep structure of the outer and Lesser Himalaya, Kumaon and Garhwal (India): Implications for evolution of the fold-and-thrust belt, *Tectonics., 13*, 89-109.

Tormann, T., S. Wiemer, and J. L. Hardebeck (2012), Earthquake recurrence models fail when earthquakes fail to reset the stress field, *Geophys. Res. Lett.*, *39*, L18310, doi:10.1029/2012GL052913.

Valdiya, K. S. (1980), Geology of the Kumaun Lesser Himalaya, *Him. Geol., 291*.

Wiemer, S., and M. Wyss (1997), Mapping the frequency-magnitude distribution in asperities: An improved technique to calculate recurrence times?, *J. Geophys. Res.: Solid Earth., 102* (B7), 15115-15128.

Wiemer, S., and M. Wyss (2000), Minimum magnitude of completeness in earthquake catalogs: examples from Alaska, the western US and Japan, *Bull Seismological Soc Am., 90*, 859-869.

Wiemer, S. (2001), A software package to analyse seismicity: ZMAP. *Seismol. Res. Lett.*, *72*(3), 373–382.

Wyss, M. (1973), Towards a physical understanding of the earthquake frequency distribution, *Geophys. J. R. Astron. Soc., 31* (4), 341-359.

Wyss, M., A. Hasegawa, S. Wiemer, and N. Umino (1999), Quantitative mapping of precursory seismic quiescence before the 1989, M 7.1 off-Sanriku earthquake, Japan, *Ann. Di Geofis.*, *42*(5), 851– 869.

X, Lei., and K Kusunose (1999), Fractal structure and characteristic scale in the distributions of earthquake epicentres, active faults and rivers in Japan, *Geophys. J. Int., 139* (3), 754-762.

Zhang, L.F., J. G. Li, W.L. Liao, and Q. L. Wang (2016), Source rupture process of the 2015 Gorkha, Nepal Mw 7.9 earthquake and its tectonic implications, *Geodesy Geodyn.,* 7(2):124–131.

[Geophysical Research Letters]

Supporting information for

[Asperity interaction and dependence of frequency-size distribution of earthquakes in brittle-ductile transition zone in Central Himalaya]

[Anil Tiwari[1, 3], Ajay Paul[1], Rakesh Singh[2], Rajeev Upadhyay[3]]

[1]Wadia Institute of Himalayan Geology, Dehradun, India

[2]Department of Earth Sciences, Graphic Era Hill University, India

[3]Department of Geology, Kumaun University, Nainital, India

Contents of this file

- Figures S1 to S7
- Tables S1 to S5

Additional Supporting Information (Files uploaded separately)

- Captions for dataset S1 to S3

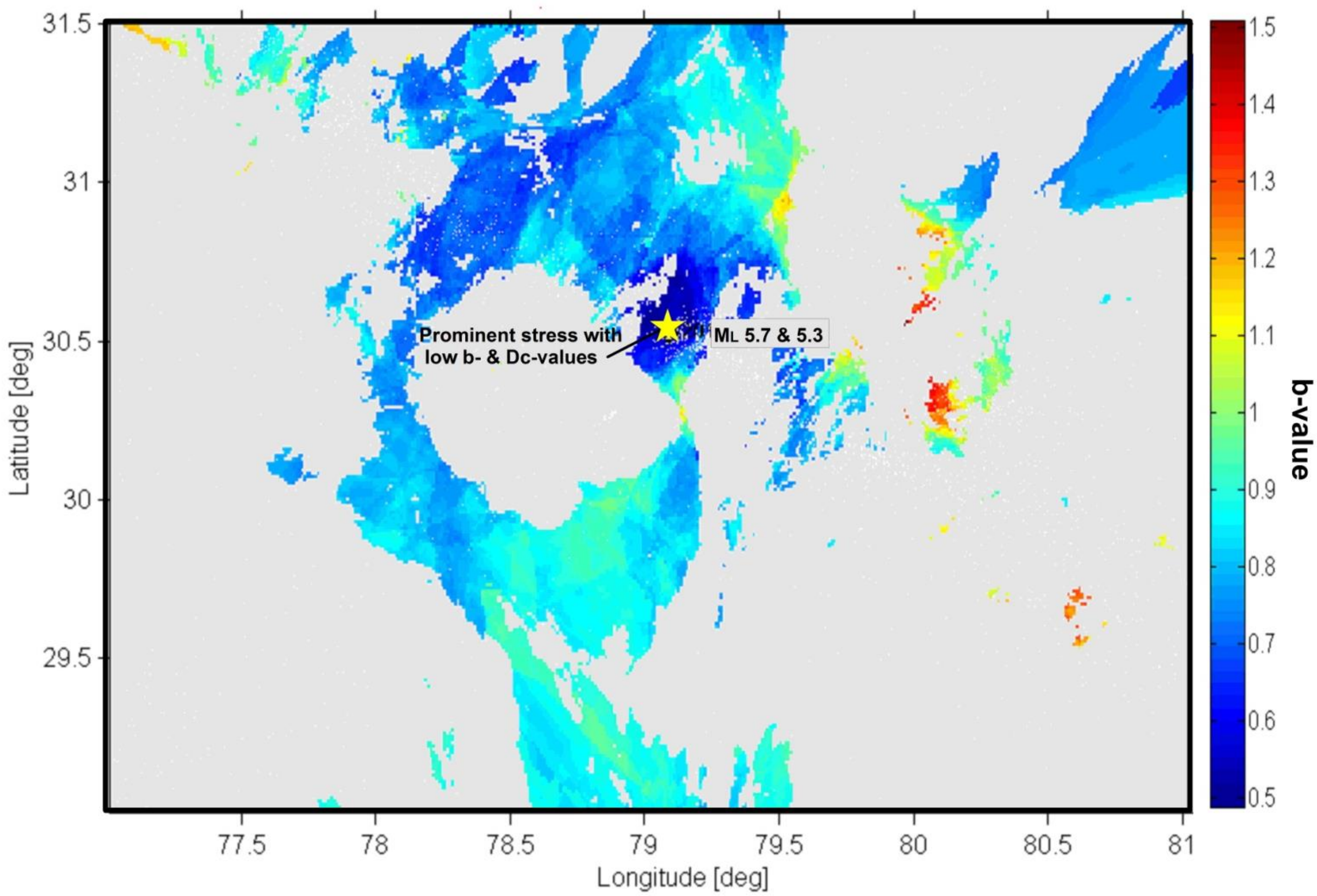

Figure S1. Figure shows b-value mapping for entire region. Yellow star depicts moderate size of earthquake in Chamoli-Rudraprayag proximity in Garhwal-Himalaya.

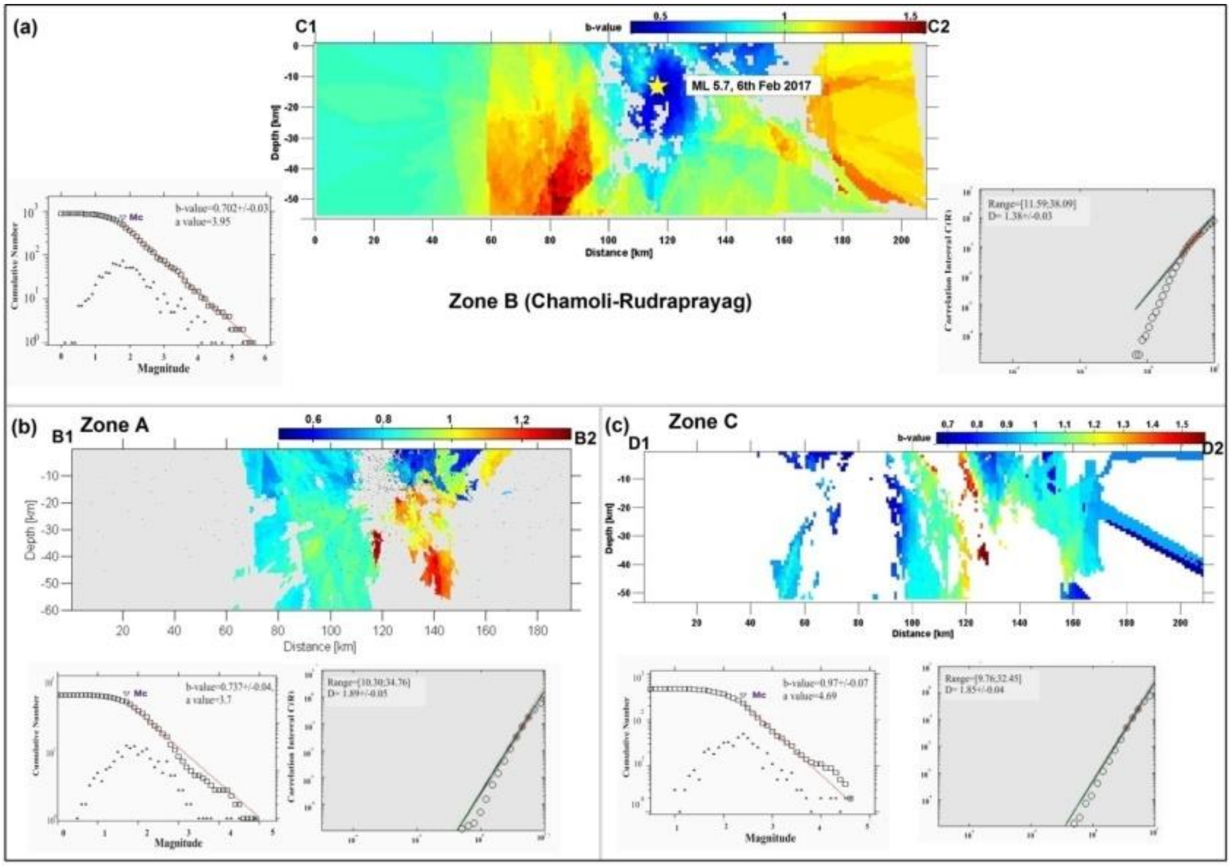

Figure S2. Figure shows (a-c) depth cross-sections of b-value (mapping across the strike) and fractal analysis in three different zones (A, B and C). The maximum magnitude recorded earthquake (M_L 5.7), since 1999, is represented by Yellow star in Zone B. The lowest b- and D_c-value in Zone B indicates high stress accumulation and significant clustering of seismic event, respectively.

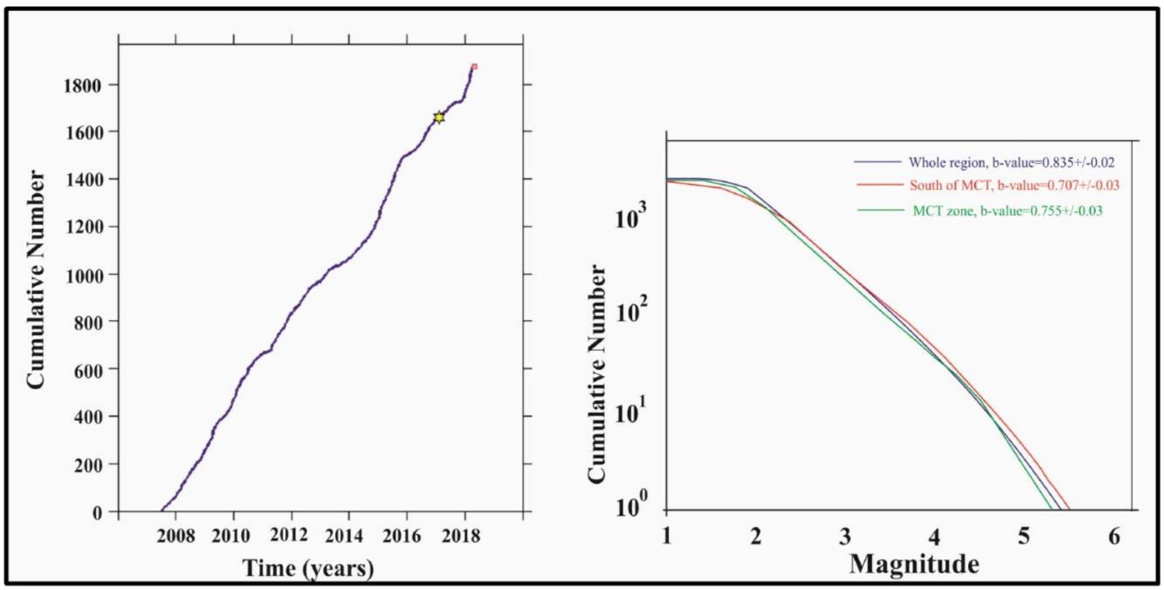

Figure S3. Spatio-temporal analysis plot: (a) cumulative frequency plot of declustered dataset of whole region. (b) shows b- value plot for whole region, MCT zone and South of MCT zone.

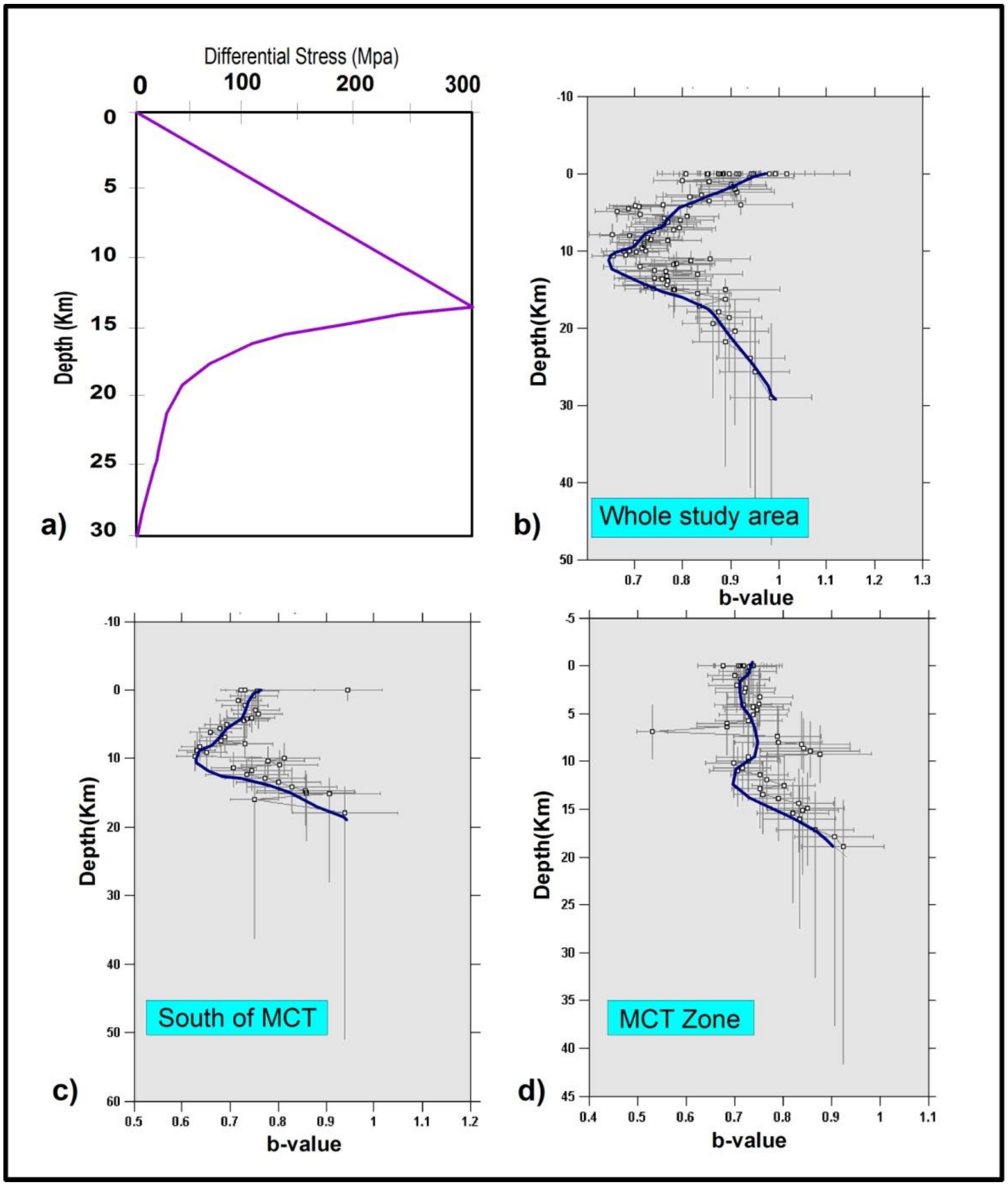

Figure S4. (a) Plot depicts depth variation of differential stress in upper crust modified after Scholz [2002]. (b-d) figures shows b- value depth variations and gradient for whole region, south of MCT zone and MCT zone, respectively.

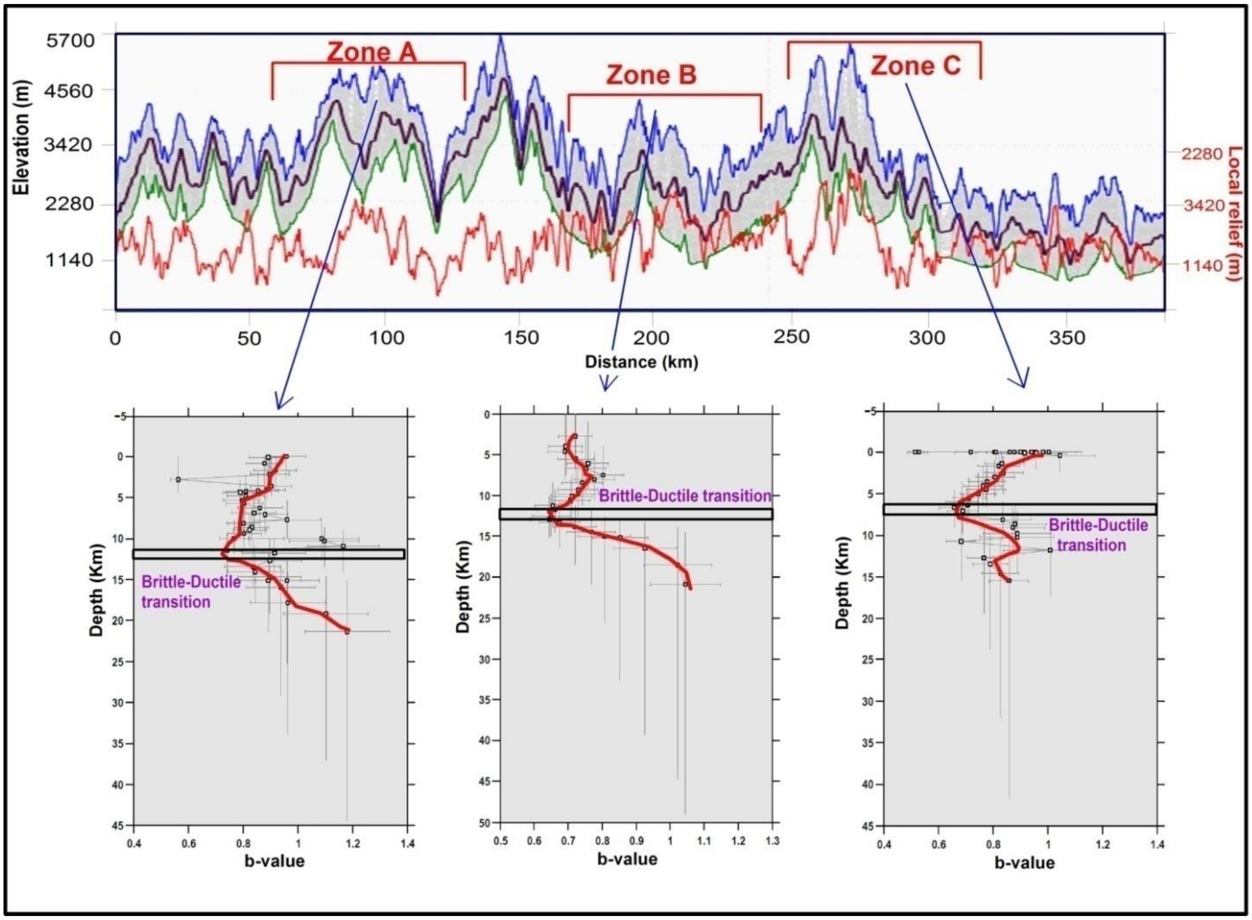

Figure S5. The swath profile along the strike shows topographic elevation varies with change in brittle-ductile contact (BDC) of zone A, B & C, depicts tectonic control on topography. Zone B shows deeper contact of BDC and low elevation above it, where as zone C shows shallow contact of BDC and highest topographic elevation is observed above zone C.

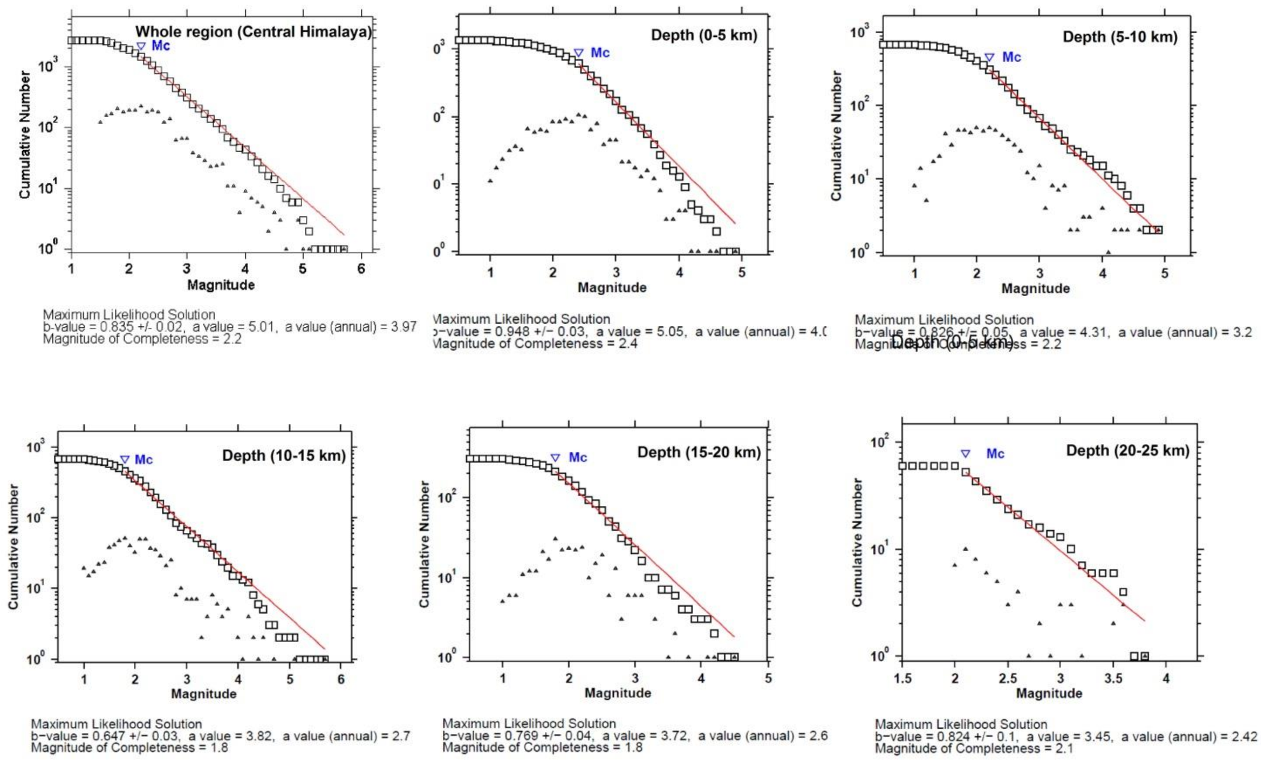

Figure S6. Output of b-values for whole region and depth wise (0-5km, 5-10 km, 10-15 km, 15-20 km and 20-25km).

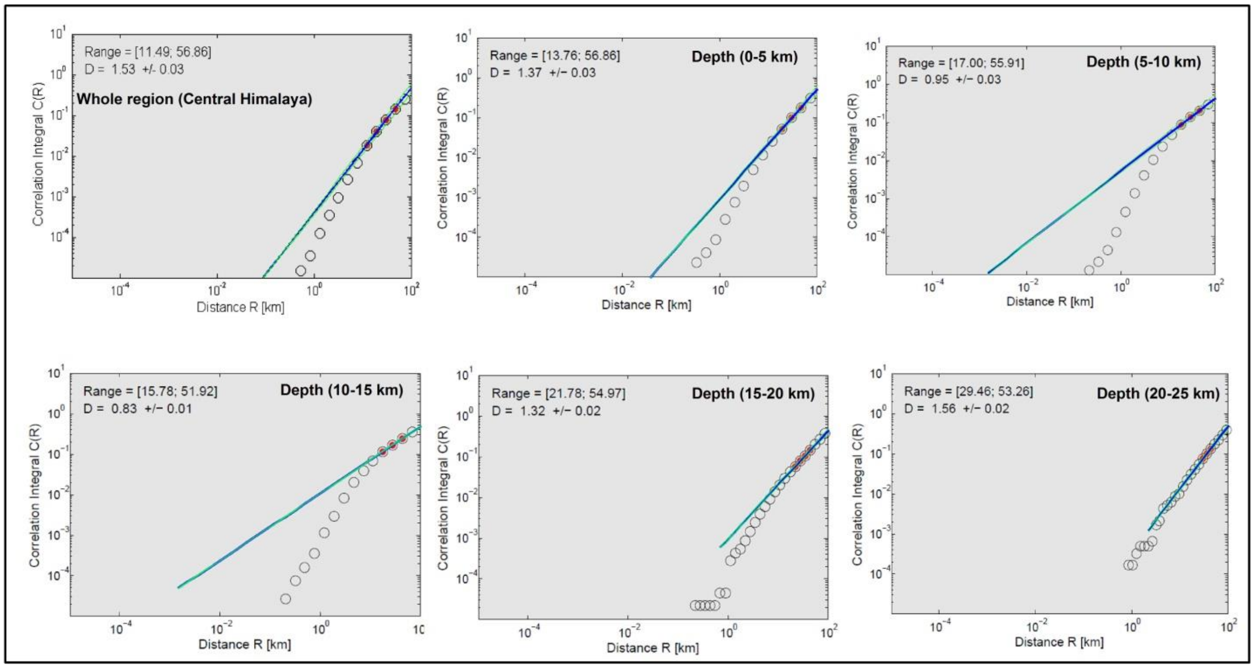

Figure S7. Output of Fractal analysis (D_c-values) for whole region and depth wise (0-5km, 5-10 km, 10-15 km, 15-20 km and 20-25km).

Table S1. Detail of seismic stations used for analysis (location, local tectonic setting and instrumentations).

S. no.	Station	Seismic Station	Lat (degree)	Long (degree)	Elevation (m)	Tectonic Zone	Sensor	Digitizer
01	Adibadri	ABI	30.15	79.21	1595	Inner Lesser Himalaya	Trillium-240	Centaur
02	Bhararisain	BSN	30.09	79.27	2258	Inner Lesser Himalaya	Trillium-120	Taurus
03	Chakrata	CKA	30.72	77.87	1990	Inner Lesser Himalaya	Trillium-240	Centaur
04	Deoband	DBN	29.72	77.73	214	Sediments of Indo-Gangetic Plain	Trillium-240	Centaur
05	Dehradun	DDN	30.33	78.01	657	Siwalik, Sub-Himalaya	Trillium-240	Centaur
06	Dhaulchina	DHA	29.67	79.79	1857	MCT zone (HHC)	Trillium-120	Taurus
07	Gaurikund	GKD	30.62	79	1760	MCT zone (HHC)	Trillium-240	Centaur
08	Guttu	GTU	30.53	78.75	1970	Inner Lesser Himalaya	Trillium-240	Centaur
09	Kotkhai	KHI	31.1	77.58	2261	HHC	Trillium-240	Centaur
10	Kharsali	KSI	30.97	78.44	2559	MCT zone (HHC)	Trillium-240	Centaur
11	Nahan	NHN	30.53	77.27	610	Siwalik, Sub-Himalaya	Trillium-240	Centaur
12	Tapovan	TPN	30.5	79.61	2110	MCT zone (HHC)	Trillium-240	Centaur
13	Munsiyari	MUN	30.07	80.26	2050	MCT zone (HHC)	Trillium-120	Taurus
14	Toli	TLI	29.81	80.37	710	Inner Lesser Himalaya	Trillium-120	Taurus

Table S2. Table shows estimated b- and D_c-values for different region by clipping the declustered dataset (according to tectonic framework and zone wise).

Sr. no	**Area**	**b_{ML}-value**	**a_{ML}-value**	**Fractal Dimension (D_c)**	**Mc**
01	**Garhwal-kumaun Himalaya (entire study area)**	0.835 ± 0.02	5.01	1.53 ± 0.03	2.2
02	**MCT Zone (along the strike)**	0.755 ± 0.03	4.38	1.46 ± 0.04	2.1
03	**South of MCT (along the strike)**	0.705 ± 0.03	3.98	1.36 ± 0.01	1.8
04	**Zone A**	0.737 ±0.04	3.7	1.89 ± 0.05	1.8
05	**Zone B**	0.702 ± 0.03	3.95	1.38 ± 0.03	1.8
06	**Zone C**	0.97 ± 0.05	4.69	1.85 ± 0.04	2.4

Table S3. Depth wise b- and D_c-values estimated in the present study for entire region in central Himalaya.

Depth Range (Km)	Fractal Dimension (D)	b_{ML}-Value	a_{ML}-Value	Mc
0-5	1.37 ± 0.03	0.948 ± 0.03	5.05	2.2
5-10	0.95 ± 0.03	0.826 ± 0.05	4.31	2.2
10-15	0.83 ± 0.01	0.647 ± 0.03	3.82	1.8
15-20	1.32 ± 0.02	0.769 ± 0.04	3.72	1.8
20-25	1.56 ± 0.02	0.824 ± 0.1	3.45	2.1

Table S4. Temporal stress level variation (2007 – 2008) for entire region. Year wise plot indicates continuous increase in stress accumulation.

Sr. no	Years	Dc	b_{ML}	M_c
01	2007-2010	1.55 ± 0.02	1.12 ± 0.05	2.2
02	2011-2014	1.39 ± 0.03	0.649 ± 0.02	1.8
03	2015-2018	1.29 ± 0.01	0.61 ± 0.02	2.0

Table S5. Detail of earthquakes $M_L \geq 4$ occurred in asperity zone coincides with low b-value zones.

S. no	Date	Origin Time (UTC: hh:mm)	Longitude (°E)	Latitude (°N)	Depth (km)	Magnitude (ML)
ZONE A						
01	2007-07-22	23:02	78.3	30.83	14	5
02	2012-02-09	19:17	78.30	30.89	14.6	4.5
03	2012-11-27	12:15	78.40	30.85	14.6	4.3
04	2013-12-25	02:57	78.34	31.04	35.6	4.2
05	2013-02-11	10:48	78.18	30.81	15	4.1
06	2016-08-18	20:05	78.19	30.89	15.9	4
07	2017-12-27	04:45	78.33	31.12	14.1	4
08	2018-02-28	05:47	78.69	30.77	13.3	4.2
Uttarkashi Eqk	1991-02-20	02:53	78.86	30.75	12	6.8 (Mw)
ZONE B						
01	2011-06-20	06:27	79.28	30.53	7	4.9
02	2013-04-06	22:29	79.03	30.61	15	4.2
03	2015-04-01	21:23	79.42	30.38	13.8	4.9
04	2015-07-18	23:48	79.11	30.49	9	4.2
05	2015-06-03	11:28	79.13	30.51	7.8	4
06	2017-12-06	15:19	79.13	30.56	13.5	5.3
07	2017-02-06	17:03	79.09	30.53	14.6	5.7
08	2017-12-28	11:17	79.12	30.53	12.5	4.7
19	2017-02-06	17:04	79.09	30.55	14.7	4.4
10	2017-02-06	17:07	79.08	30.54	10.5	4
11	2017-04-07	13:03	79.24	30.54	11.5	4
12	2017-08-22	12:02	79.53	30.50	12.1	4
13	2018-01-05	20:55	79.12	30.54	11.7	4.5
14	2018-01-08	04:04	79.19	30.50	11.8	4.2
Chamoli Eqk	1999-03-28	05:18	79.21	30.38	15	6.6 (Mw)
ZONE C						
01	2010-05-01	22:36	80.15	30.146	10.8	4.6
02	2010-07-06	19:08	80.46	30.081	8.1	5.1
03	2010-06-22	23:14	80.44	30.112	6.2	4.3
04	2010-07-04	02:35	80.45	30.12	5.5	4.3
05	2010-02-22	17:23	80.12	30.123	10.1	4.2
06	2015-09-29	09:27	80.15	30.141	17.3	4.5
07	2016-12-01	16:52	80.53	29.965	8.8	5.0
08	2016-06-07	20:10	80.14	30.056	8.6	4.4
09	2018-04-01	15:11	80.13	30.029	7.9	4.2
10	2018-03-16	15:41	80.16	30.132	9	4

- **Dataset S1.** Original data magnitude ranges from M_L 1 to 5.7.
  (Dataset format: Longitude, Latitude, Year, Month, Day, Magnitude, Depth, Hour and Minute)

- **Dataset S2.** Declustered earthquake dataset (M_L 1.8 -5.7), aftershock removed using the Reasenberg [1985] algorithm in csv format.
  (Same format as dataset S1)

- **Dataset S3.** Declustered earthquake dataset (M_L 1.8 -5.7), aftershock removed using the Gardner and Knopoff [1974] algorithm in csv format.
  (Same format as dataset S1)